Indonesian Journal of Chemical Research

http://ojs3.unpatti.ac.id/index.php/ijcr Indo. J. Chem. Res., 9(1), 26-34, 2021

Recovery of Gold in Au/Cu/Mg System from SH/Fe_3O_4@SiO_2 as a Magnetically Separable and Reusable Adsorbent

Ani Qomariyah[1,2*], Nuryono[2], Eko Sri Kunarti[2]

[1]Study Program of D4 Medical Laboratory Technology, Institute of Health Science Banyuwangi, East Java 68400, Indonesia
[2]Chemistry Departement, Mathematics and Natural Sciences Faculty, Universitas Gadjah Mada, Yogyakarta 55281, Indonesia
[*]*Corresponding Author: ani.qomariyah@stikesbanyuwangi.ac.id*

Received: February 2021
Received in revised: March 2021
Accepted: May 2021
Available online: May 2021

Abstract

The recovery of Au(III) in the Au/Cu/Mg system from mercapto-silica hybrid coated magnetite (SH/Fe_3O_4@SiO_2) adsorbent has been investigated. This adsorbent characterized using FT-IR to determine functional groups, crystallinity study using XRD, surface morphology using SEM, material compositions with XPS, surface area using nitrogen adsorption, and TGA to study thermal stability. Adsorption of metal ions carried out with batch system for 30 minutes at a pH of 3. In the Au/Cu/Mg multi-metal system, Au(III) ions were easily desorbed (approximately 85%) by SH/Fe_3O_4@SiO_2 adsorbent based on HSAB (Hard Soft Acid Base) theory that Au(III) ion is a softer metal than Cu(II) and Mg(II) where Au(III)>Cu(II)>Mg(II). The recovery of Au(III) ions was easily desorbed using thiourea 7% in 0,1 M HCl solution with the percentage of 79%. The process of SH/Fe_3O_4@SiO_2 adsorbent separation after adsorption and recovery was very easy. The adsorbent could perfectly separate in 5 minutes using an external magnet. The SH/Fe_3O_4@SiO_2 adsorbent can be reused on the adsorption-desorption process of Au(III) in the Au/Cu/Mg system approximately four times of cycle reactions.

Keywords: Magnetite, silica, recovery, Au(III), thiourea

INTRODUCTION

The world's need for gold is currently increasing in line with technological advances, general intelligence, and experience in gold ore processing. Gold is one of the mineral resources which are once taken and will run out (non-renewable resources) and cannot be renewed or recovered. Gold exploration areas in the world include Africa, China, America, Australia, and Indonesia. These areas are the main focus of gold-producing companies. The relative abundance of gold in the earth's crust is estimated at 0.004 g/tonne, including about 0.001 g/ton in marine waters (Umaningrum, Mulyasuryani, & Sulistyarti, 2016). Gold has high economic benefits for individuals, groups, and countries. The economic potential is seen from mining activities on a large scale and reaching national distribution at a high selling price (Arifya & Afdal, 2020).

The gold isolation method widely used is the cyanide method and the amalgamation method (Ekmekyapar, Aslan, Bayhan, & Cakici, 2012). Many people are unaware that mercury and cyanide can settle on riverbeds and enter the food chain when they enter the human body through water and river products used by humans. This situation results in the accumulation of heavy metals in human tissue to slowly cause permanent damage to organs and chronically lead to death.

These methods are also not very environmentally friendly because they cause environmental damage and threaten human survival. Therefore, it is necessary to develop an effective and efficient, and environmentally friendly method to separate gold from other metal alloys, such as Cu, Ag, Fe, Zn, Mg, Co, Ni, Pb, and Mn. Another alternative method that can be used is the adsorption method (Bijang, Latupeirissa, & Ratuhanrasa, 2018). This method is easy to operate, simple, and large (Powell et al., 2007).

Various gold adsorption methods have been developed to obtain adsorbents with high thermal and mechanical stability, large surface area, and easy modification. One of the adsorbents that are widely used as inorganic solids is silica gel. Silica gel has the functional groups of silanol (-Si-OH) and siloxane (Si-O-Si) to adsorb transition metal ions. Silica gel has been modified with various types of functional groups to become more efficient, such as amines, thiol, and sulfonates (Manuhutu, Nuryono, & Santosa, 2018) for the adsorption of various types of metal ions. Since

Au(III) belongs to the category of soft acids, the modified silica gel with the thiol group (-SH) as a soft base (Ngatijo, Gusti, Fadhilah, & Khairunnisah, 2020) is expected to be able to effectively adsorb gold metal ions based on the HSAB (*Hard Soft Acid Base*) concept.

The purpose of separating the filtrate from adsorption and desorption; so far, the method developed is filtering (Powell et al., 2007). Although this method is easy to do, it is less efficient because it takes a long time. Therefore, it is necessary to look for other, more straightforward methods. Another alternative method that has been developed is separation by applying an external magnetic field (Nuryono et al., 2019). In this method, the modified silica adsorbent can be separated directly by exerting a magnetic influence from the outside because the adsorbent is magnetic. One of the magnetic materials is the oxide of the transition metals (Rahmayanti, Santosa, Sutarno, & Paweni, 2021)

Among the transition metal oxides, iron oxide is an exciting material to study. Naturally, these metal oxides are found in the form of iron oxide minerals. Iron oxide minerals are in the form of magnetite (Fe_3O_4), maghemite (γ-Fe_2O_3), and hematite (α-Fe_2O_3). The difference in calcination temperature results in various forms of the iron oxide phase, where Fe_3O_4 occurs at room temperature, γ-Fe_2O_3 in 200 $^{\circ}$C and α-Fe_2O_3 in 300-600 $^{\circ}$C (Manuhutu et al., 2018). Modification of the magnetite layer must produce adsorbents with high adsorption effectiveness (Mujiyanti, Nisa, Rosyidah, Ariyani, & Abdullah, 2020). Therefore, in this study, magnetite coating was carried out with mercapto-modified silica from 3-mercaptopropyl trimethoxysilane (MPTMS). The result yielded a coated magnetite adsorbent mercapto-silica hybrid ($SH/Fe_3O_4@SiO_2$). In addition to producing adsorbents with high adsorption effectiveness, the filtrate separation process will be easier to do.

Desorption is carried out to release the metal-bound to the adsorbent. According to Lacoste-Bouchet, Deschênes, & Ghali, (1998), gold desorption or leaching in industry and mining generally uses cyanide as a desorption solution. Still, cyanide has many disadvantages, including being unfriendly to the environment and dangerous to human health so that its use is limited. This disadvantage has led to the development of eluents that are more environmentally friendly and harmless to humans. Hidayati, Suyanta, & Santosa, (2018) using glutamic acid for reductive desorption [$AuCl_4^-$] adsorbed on magnetite Mg/Al-NO_3. Mulyasuryani, Ismuyanto, & Purwonugroho, (2012) using Potassium Thiocyanate (KSCN) for gold desorption adsorbed on activated carbon from coconut shell charcoal, while Adha, (2015) using the HNO_3 solution. In addition, Na_2EDTA can also be used as a gold desorbing agent (Sa'adah, Zaharah, & Shofiyani, 2018)

In this research, the characteristics of the adsorbent material were studied $SH/Fe_3O_4@SiO_2$, then used for adsorption and studied about the desorption kinetics of Au (III) ions in a multi-metal system for Au/Cu/Mg.

METHODOLOGY

Instrumentals and Materials

This study uses analytical tools and supporting equipment. For analysis, the equipment used scanning electron microscopy (HITACHI, S-4800), X-ray diffractometer (Shimadzu XRD-6000, Cu kα with voltage 40 kV and current 30 mA), *X-ray photoelectron spectra* (Rigaku XPS-7000 with Mg Kα radiation), nitrogen adsorption / BET (BEL Japan Inc., gas flow of N_2 at 150 $^{\circ}$C for two hours), *thermo gravimetric analysis* (TGA) using Thermo Plus 2 TG-DTA TG8120, infrared spectrophotometer (Shimadzu FTIR Prestige21), and atomic absorption spectrophotometer (contrAA 300). As supporting equipment includes analytical scales (Mettler AE 160), oven (WTC Binder), external magnet, micropipette 1000 µm, shaker (VRN-200), sonicator (Bransonik 220 with frequency 48 kHz), pH meter (Horiba F-52), porcelain cup, grinding tool (lumping 40 and mortar), glassware and plastic utensils.

The materials used to synthesize coated magnetite are $FeCl_2$•$4H_2O$, $FeCl_3$•$6H_2O$, HCl 37%, and NH_4OH 25% obtained from the brand, mineral water obtained from the Universitas Gadjah Mada, Food and Nutrition Laboratory. As a comparison, it is used Fe_3O_4 95% from Aldrich. For the source of silica, a Na_2SiO_3 solution is used from the destruction of rice husk ash. Mercapto group (-SH) taken from 3-merkaptopropiltrimetoksisilan (MPTMS) obtained from Merck. For the adsorption process used $HAuCl_4$ solution (Analytical Chemistry Laboratory, Faculty of Mathematics and Natural Sciences UGM) with concentration 500 mg/L, $CuCl_2$•$2H_2O$ (Merck), buffer solution with pH 2-7. For desorption, the thiourea solution was used (Merck), HCl 0,1 M from HCl 37 % (Alba Chemical), Na_2EDTA (Merck), glutamic acid (Merck), and HNO_3 Solution (Merck).

Procedure

Magnetite Synthesis

A total of 5.2 grams of $FeCl_3.6H_2O$ and 2 grams of $FeCl_2.4H_2O$ were mixed with 1 mL of 37% HCl.

Then 200 mL of demineralized water was added to the mixture. Then the solution was sonicated, and N_2 gas flowed for 1 hour. During sonication and flow of N_2 gas, 15 mL of 25% NH_3 solution is added dropwise to form black colloid magnetite. After the sonication process and N_2 gas flow were completed, the magnetite colloid was left to stand for 24 hours. The magnetite colloid was washed with 200 mL of demineralized water flowed with N_2 gas for 5 minutes. The washing process is carried out three times. The magnetite formed was dried in an oven at 80 ºC until dry, then characterized by XRD, XPS, FT-IR, SEM, and N_2 adsorption.

Magnetite coating with silica and MPTMS

A total of 0.5 grams of magnetite was put into a PET glass and acidified with 1 mL of 1 M HCl. Then the acid solution was separated from the magnetite with the help of an external magnetic field. 3 mL of sodium silicate and 2.36 mL of demineralized water were added to the acidified magnetite and then sonicated for 5 minutes. Furthermore, 0.63 mL of MPTMS solution was added to the magnetite and sodium silicate mixture, which had been sonicated and then stirred. 1 M HCl solution or 1 M NH_4OH solution is added dropwise while stirring until it forms a gel or pH 7. The gel formed is dried in an oven at 80 ºC. The results are mashed and washed with demineralized water until a neutral pH. After washing, the coated magnetite was dried again at 80 ºC for 24 hours to obtain SH/Fe_3O_4@SiO_2 (coated magnetite mercapto-silica hybrid). The SH/Fe_3O_4@SiO_2 material was characterized using XRD, XPS, FT-IR, SEM, and N_2 adsorption.

Adsorption of Au(III), Cu(II), and Mg(II) metals with SH/Fe_3O_4@SiO_2

Adsorption of Au(III) with SH/Fe_3O_4@SiO_2 adsorbent was carried out at variations of pH = 1, 2, 3, 4, 5, 6, and 7.A 20 mg of SH/Fe_3O_4@SiO_2 adsorbent was added with 100 mg/L of Au (III) solution with varying pH. Adsorption was carried out for 30 minutes, then the filtrate was separated with an external magnet, and AAS analysis was carried out to determine the concentration of Au(III) adsorbed. The same step is carried out for the adsorption of Cu(II) and Mg(II) metals.

Adsorption of Au (III), Cu (II), and Mg (II) metals in a multilateral Au/Cu/Mg system

Adsorption of mixtures of Au(III), Cu(II), and Mg(II) with SH/Fe_3O_4@SiO_2 adsorbent was carried out at variations of pH = 3. A total of 20 mg of adsorbent SH/Fe_3O_4@SiO_2 were added with a solution of Au(III), Cu(II), and Mg(II) 10 mL each with a concentration of 100 mg/L each. Adsorption was carried out for 30 minutes, then the filtrate was separated with an external magnet, and AAS analysis was carried out to determine the concentration of Au (III), Cu (II), and Mg \(II) adsorbed.

Desorption of Au (III) in the Au/Cu/Mg mixture from SH/Fe_3O_4@SiO_2

Adsorbed Au(III), Cu(II), and Mg(II) ions are desorbed with various desorbing solutions. This study used a solution of thiourea in 0.1 M HCl, 0.1 M Na_2EDTA, 0.1 M glutamic acid, and 0.1 M HNO_3 solution. The effect of thiourea concentration was also studied by varying the concentration of thiourea 3%, 5%, and 7%. Desorption kinetics were studied by varying the desorption time, namely 5, 20, 30, 60, 90, and 120 minutes. After desorption, the filtrate was separated with an external magnet and analyzed by AAS to determine the concentration of each metal that was successfully desorbed.

RESULTS AND DISCUSSION

Synthesis of the SH/Fe_3O_4@SiO_2 adsorbent

In this study, magnetite was synthesized through a coprecipitation technique. This technique using NH_4OH solution as a precipitator and ferrous chloride salt as a Fe^{2+}/Fe^{3+} source. The ultrasonic stirring technique was used, and a black magnetite precipitate was formed when the NH_4OH solution was added to the Fe^{2+}/Fe^{3+}solution. In magnetite synthesis, Fe^{2+}: Fe^{3+} molar ratio all it takes is 1: 2 according to the following reaction equation:

$$Fe^{2+}_{(aq)} + 2Fe^{3+}_{(aq)} + 8OH^-_{(aq)} \rightarrow Fe_3O_{4(s)} + 4H_2O_{(l)}$$

Nitrogen gas is needed when synthesizing magnetite to prevent oxidation reactions. The oxidation reactions that are possible to occur in magnetite follow the following equation:

$$4\ Fe_3O_{4(s)} + O_{2(g)} + 18H_2O_{(l)} \rightarrow 12\ Fe(OH)_{3(s)}$$

The following shows the yield of magnetite synthesis results and the weight of coated magnetite in Table 1 below.

Table 1. The yield of synthesized magnetite and weight of magnetite coating

Fe_3O_4 Synthetic		SH/Fe_3O_4@SiO_2	
Yield weight (g)	2.24	Before coating (g)	1.00
Yield (%)	96.55	After coating (g)	1.90

From Table 1, the yield of magnetite is quite high.

This result follows previous research (Ngatijo et al., 2020), while the synthesis of magnetite by mechanical stirring was obtained the smaller yield, namely 94.40%. In this study, the ultrasonic stirring technique was used. Synthesis of magnetite with ultrasonic stirring obtained higher yields (greater than 95%) because the energy from ultrasonic waves can make contact between iron ions and hydroxide ions more effective in forming the iron hydroxide. Iron hydroxide will undergo a further reaction to obtain magnetite, like the reaction below.

$$12\ Fe(OH)_{3(s)} \rightarrow 4\ Fe_3O_{4(s)} + O_{2(g)} + 18H_2O_{(l)}$$

SH/Fe_3O_4@SiO_2 Adsorbent characterization with Scanning Electron Microscopy (SEM)

Figure 1b shows that Fe_3O_4@SiO_2 still maintaining the morphological properties of Fe_3O_4 (Figure 1a), and a smoother surface structure is obtained, where the silica is uniformly coated on the magnetite particles. The particle sizes uniformity of magnetite and coated magnetite was proven by measuring the diameter of each particle. In this study, the particle diameter was then determined by the average using Image-J software. The average diameter of the magnetite particles was 11 nm. The average diameter of the magnetite particles coated with silica was 21 nm. These two results came from selecting 150 particles.

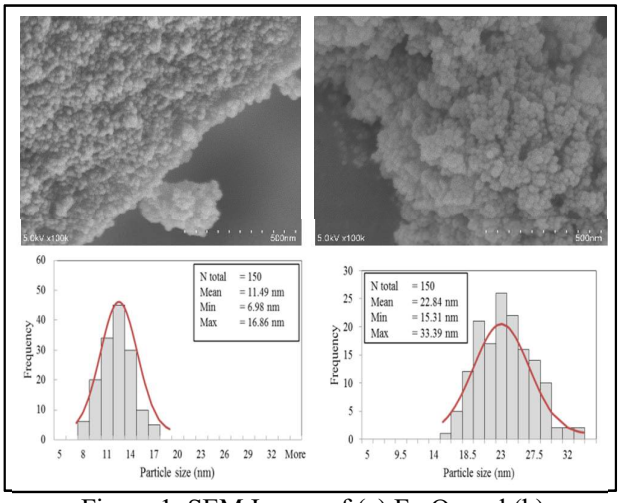

Figure 1. SEM Image of (a) Fe_3O_4 and (b) Fe_3O_4@SiO_2

Due to the average diameter of the magnetite and Fe_3O_4@SiO_2 obtained, the thickness of the silica can be determined to be about 5 nm. A hypothetical model of silica thickness at Fe_3O_4@SiO_2 can be illustrated in Figure 2.

X-Ray Diffractometry (XRD)

The success of magnetite synthesis is shown by the XRD diffractogram (Figure 3), where the Fe_3O_4 peaks appear at 2θ, the same as the coated magnetite. The synthesized magnetite yields the highest peak at 35.99° with an index [311]. This peak index also occurs in coated magnetite. Other magnetite peaks appear at 29.67°, 43.43°, 54.98°, and 63.82° respectively, indicating the indexes [220], [400], [422], and [440].

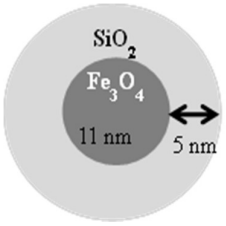

Figure 2. Hypothetical model of silica thickness at Fe_3O_4@SiO_2

The silica-coated magnetite peaks appear to widen due to the silica's amorphous phase, which shows Fe_3O_4@SiO_2 has a semi-crystalline structure. The amorphous phase of silica can improve the adsorption performance based on previous research (Ngatijo et al., 2020). The magnetite plating process does not change position [311]. This condition means that the plating process does not damage the crystal structure, but this process only reduces the intensity of the magnetite. In the XRD analysis, the reduced intensity of the magnetite after coating the silica. This situation shows that the silica has been completely coated on the magnetite surface. Finally, the magnetite detected by the XRD device decreases in intensity (Kurnia, Kaseside, & Iwamony, 2021).

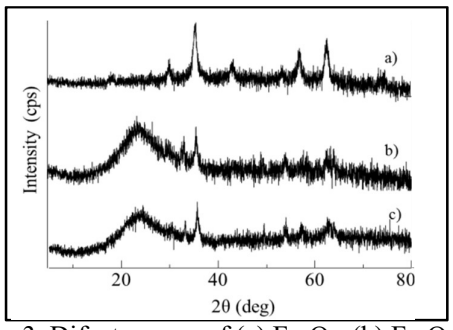

Figure 3. Difactrogram of (a) Fe_3O_4, (b) Fe_3O_4@SiO_2 and (c) SH/Fe_3O_4@SiO_2

Fourier-Transform Infrared Spectrometry(FT-IR)

An absorption band indicates the characteristic absorption of the magnetite Fe-O bond. The magnetite Fe-O bonds are in the intermediate wavenumber region

at 355-370 cm^{-1} and 560-580 cm^{-1}. The absorption of the magnetite Fe–O bond decreases in intensity after coating. This absorption occurs because the surface of the magnetite is covered by coatings, both silica and MPTMS. The reduced intensity of Fe–O absorption indicates the more perfect the coating is formed. These results are in line with SEM and XPS analyses. The success of the magnetite coating process with silica and MPTMS from SEM analysis is known by the increase in particle diameter (Figure 1). Whereas in the analysis using XPS, Fe2p peaks did not appear in silica-coated magnetite or MPTMS (Figure 5).

The magnetite coating process was carried out using the sol-gel method. In this method, a polymer is formed from Si so that there is a siloxane bond (Si–O–Si) on coated magnetite. The success of this polymer formation was observed in the spectra of the coated magnetite. The Si–O–Si bending vibration is indicated by the absorption band in the wavenumber region 463 cm^{-1}. Asymmetric stretching vibrations and symmetry of the Si–O–Si bonds are observed in the wavenumber region 802 cm^{-1} and 1072 cm^{-1}. The absorption band appears in the wavenumber area of 3441 cm^{-1}, and 1636 cm^{-1} in the coated magnetite spectra is the absorption band from stretching vibrations and bending vibrations of the –OH groups from the Fe–OH and Si–OH bonds.

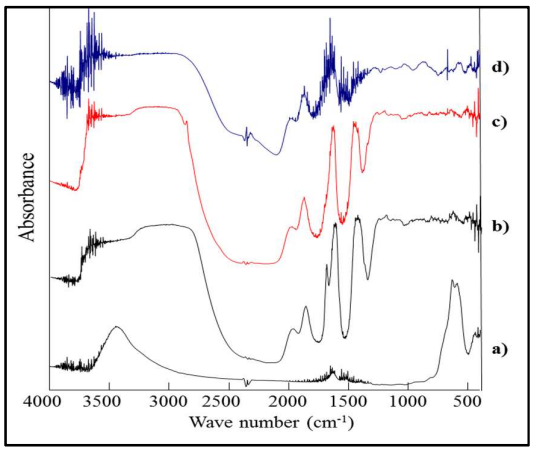

Figure 4. FT-IR Spectra of (a) Fe_3O_4, (b) Fe_3O_4@SiO_2, (c) SH/Fe_3O_4@SiO_2 and (d) Au/SH/Fe_3O_4@SiO_2

The absorption of siloxane groups (Si-O-Si), silanol (Si-OH), and hydroxyl (–OH) indicate that magnetite has been coated with silica. The stretching vibration of the Si–O–H bond resulted in the appearance of an absorption band in the area of wave numbers 950-960 cm^{-1}. Fe_3O_4@SiO_2 uptake from the Si-OH vibration was not observed because it overlapped with the width of the absorption band from the Si–O–Si stretching vibration. Compared with the FTIR spectra of magnetite, the spectra of coated magnetite with mercapto-silica hybrids (SH/Fe_3O_4@SiO_2) have a characteristic absorption band in the form of vibrations propyl groups and mercapto groups (–SH) originating from MPTMS.

The presence of the propyl group results in the appearance of an absorption band in the region of wave number 1404 cm^{-1} which is the bending vibration of –CH_2–. The C–H bond on the propyl group results in absorption at wave number 2932 cm^{-1} as an asymmetric stretching vibration, while the absorption band for the –SH group will appear at wave number 2600-2450 cm^{-1}. Based on Figure 4, a weak absorption band appears at 2569 cm^{-1} which indicates the absorption band for the –SH group. In addition, the mercapto group (–SH) was also identified in the region of the wavenumber 694 cm^{-1}, which is the asymmetric stretching vibration of C–S.

X-Ray Photoelectron Spectroscopy (XPS)

The purpose of differentiating among the synthesized materials and identify their composition, the surface structure was further analyzed using XPS. Before analyzing the results of the XPS spectra, a correction is required for the binding energy of the carbon atom. The highest bond energy in carbon analysis is 268.7 eV. Then, a peak correction of 1.9 eV is obtained by calculating the difference in the reference carbon binding energy (284.8 eV). Figure 5 shows the Fe 2p region of magnetite and modified magnetite. As shown in Figure 3a, the main peaks appear at 709.0 eV ($2p_{3/2}$) and 723.5 eV ($2p_{1/2}$), indicating that the Fe atom exists as Fe_3O_4. These results are consistent with the literature(Márquez et al., 2012) (Marquez et al., 2011). These two peaks did not appear in all coated magnetite samples (Figs. 5b, 5c, and 5d). This condition shows that the entire surface of the magnetite has been coated with silica.

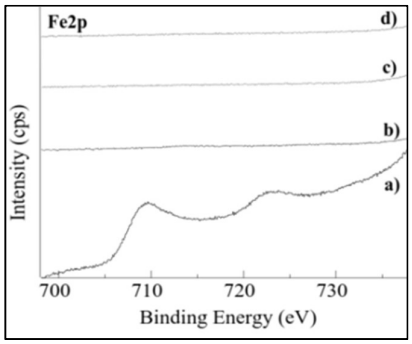

Gambar 5. XPS Spectra of Fe 2p (a) Fe_3O_4, (b) Fe_3O_4@SiO_2, (c) SH/Fe_3O_4@SiO_2, and (d) Au/SH/Fe_3O_4@SiO_2

Nitrogen Adsorption

The adsorption-desorption isotherms of magnetite and modified magnetite are represented in Figure 6. The figure shows that the three samples show different curves.

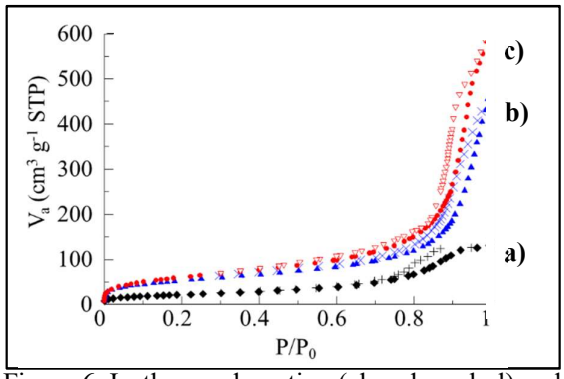

Figure 6. Isotherm adsorption (closed symbol) and isotherm desorption (open symbol) of (a) Fe_3O_4, (b) Fe_3O_4@SiO_2, and (c) SH/Fe_3O_4@SiO_2

The lowest volume of nitrogen gas adsorbed on magnetite is due to the non-porous character of the magnetite. After coating with MPTMS, the volume of nitrogen gas adsorbed on the surface of the magnetite decreased slightly, and a decrease followed this in the surface area of the BET. This condition is probably due to the reduction of silica pores after coating with MPTMS. Additionally, the graph depicts small hysteresis loops showing capillary condensation and evaporation of mesoporous silica material. Thus, it can be determined that the silica-coated magnetite adsorbent has a type V type N_2 isotherm (Anovitz & Cole, 2015).

Thermo Gravimetric Analysis (TGA)

Thermo/thermal Gravimetric Analysis (TGA) is used to study the thermal stability of magnetite and silica materials. The TGA curve is divided into several regions based on different ranges of lost mass. The TGA profile for magnetite (Figure 7a) shows three regions of lost mass. The first region at 25-100 ºC represents removal from physically absorbed water. At temperatures between 100-250 ºC is the thermal stability of magnetite. Above 250 ºC, removal of residual chemical compounds begins.

Based on Figures 7b, 7c and 7d depict the TGA profiles of silica-coated magnetite and mercapto-silica modified magnetite. The curves represent three areas of mass loss. The first region at 25-100 ºC is due to removing physically absorbed water, which will end up entirely in temperatures between 110 and 150 ºC. At a temperature of 150-250 ºC, the material is in a stable state.

Above 250 ºC (Figure 7b), condensation of the vicinal hydroxyl groups begins, leaving siloxane groups.

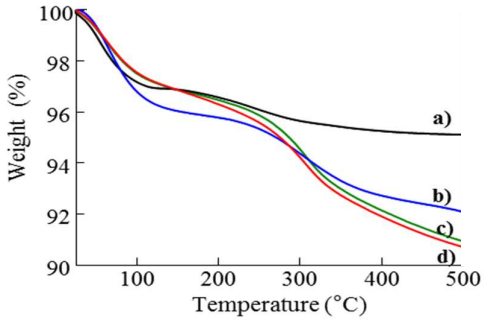

Figure 7. TGA profile of (a) Fe_3O_4, (b) Fe_3O_4@SiO_2, (c) SH/Fe_3O_4@SiO_2, and (d) Au/SH/Fe_3O_4@SiO_2

This process nearly ends up to 500-600 ºC. Figures 7c and 7d above 200 ºC may be due to removing residual organic compounds such as toluene and methanol.

Recovery Au(III), Cu(II), Mg(II), and mixture Au/Cu/Mg

Based on Figure 8, it can be seen that the average percentage of metal ions Au (III), Cu (II), and Mg (II) will show stable results in the pH range = 2-4. Au (III) species at pH = 2-5 are in the form Au^{3+} while at higher pH, they are present as $[Au(OH)_2]^-$ which causes a decrease in the percentage of adsorption of Au (III) ions against the thiol (-SH) group of SH/Fe_3O_4@SiO_2 adsorbent. The Cu (II) ion that can be adsorbed at pH = 2–5 is 40%. Changes in pH at pH = 2–5 did not affect the percentage of Cu (II) adsorbed, while at pH = 6–7, there was a decrease in the percentage of adsorbed Cu(II) to about 15%.

This number is due to the ability of the sulfur (S) atom of the thiol (-SH) functional group to chelate the Cu(II). This condition is influenced by the type of Cu (II) species where at pH = 2–5 it is as Cu^{2+}, at pH=6 already began to form $CuOH^+$ species and $Cu(OH)_2$ species began to form at pH= 7 (Powell et al., 2007). The presence of $CuOH^+$ and $Cu(OH)_2$ species indicates that Cu (II) is deposited so that Cu(II), which the SH/Fe_3O_4@SiO_2 adsorbent can adsorb, is decreasing.

Meanwhile, Mg (II) ion in the low and high pH ranges is almost entirely adsorbed slightly on the adsorbent due to its complex structure. Therefore, in this study, pH=3 was chosen as the reaction condition for the adsorption and desorption of Au (III), Cu (II), and Mg (II) metals.

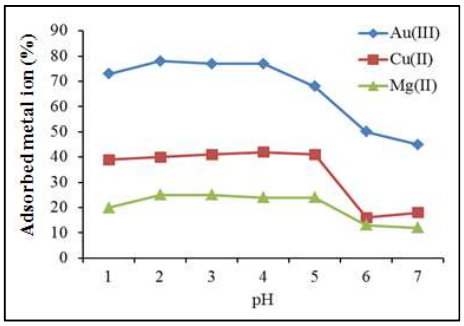

Figure 8. The effect of pH variation on the percentage of adsorbed Au (III), Cu (II), and Mg (II) metal ions

From Table 2, in the Au/Cu/Mg mixed system, the number of adsorbed Au(III) ions shows a much greater value when compared to the number of Cu(II) and Mg(II) ions that can be adsorbed. This condition is following the concept of HSAB (Hard Soft Acid and Base) where Au (III) is a soft acid so that it can form a more stable complex with the active site of $SH/Fe_3O_4@SiO_2$ (–SH group), which is also a soft base.

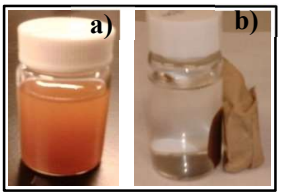

Figure 9. Adsorbent separation (a) before and (b) after use of an external magnet for 5 minutes

The separation of the adsorbent from the adsorbate is effortless and practical. The adsorbent can only be separated in about 5 minutes (Figure 9). In the gold recovery process, the thiourea solution with HCl addition will stabilize and prevent the thiourea from degrading, thereby reducing thiourea consumption. Chloride ion (Cl^-) which comes from the addition of HCl to function as a competing agent or competitor for the complex $[AuCl_4]^-$ on the $SH/Fe_3O_4@SiO_2$ surface so that gold, copper, or magnesium will be released from the surface of $SH/Fe_3O_4@SiO_2$ (Ertan & Gülfen, 2009).

In addition, in solution, ligands with large donor atoms such as S limit their ability to form stable complexes with smaller metal atoms. Complexes created with smaller atoms will cause the coordination number of metal ions to be lower than they should be because the metal ions have to make room for the larger donor atoms. Au> Cu> Mg is based on the atomic size so that Au will form a more stable complex than Cu, and Mg, Cu will form a more stable complex than Mg.

Table 2. The number of metal ions desorbed on the adsorbent in the Au/Cu/Mg multi-metal system

Absorbing Agent	Number of Metal Ions	Au(III)	Cu(II)	Mg(II)
Thiourea 7% in 0.1 M HCl	adsorbed (mg)	2.40	1.25	1.20
	desorbed (mg)	2.01	0.98	0.97
	% desorbed	79.05	58.21	48.22
Thiourea 5% in 0.1 M HCl	adsorbed (mg)	2.40	1.24	1.20
	desorbed (mg)	1.58	0.75	0.60
	% desorbed	71.20	52.20	41.00
Thiourea 3% in 0.1 M HCl	adsorbed (mg)	2.40	1.25	1.21
	desorbed (mg)	1.01	0.48	0.43
	% desorbed	58.02	40.08	35.12
0.1 M Na_2EDTA	adsorbed (mg)	2.41	1.26	1.20
	desorbed (mg)	0.79	0.29	0.21
	% desorbed	29.05	33.06	18.26
0.1 M Glutamic acid	adsorbed (mg)	2.40	1.25	1.21
	desorbed (mg)	0.45	0.18	0.12
	% desorbed	26.21	30.04	16.02
0.1 M HNO_3	adsorbed (mg)	2.41	1.25	1.20
	desorbed (mg)	0.40	0.11	0.06
	% desorbed	17.67	25.21	11.20

*The weigh of $SH/Fe_3O_4@SiO_2$ = 20 mg

In desorption using Na_2EDTA, glutamic acid, and HNO_3, positively charged amine groups can attract $[AuCl_4]^-$ and various other metal ions, which are also negatively charged in solution. Au(III) metal ions also transfer electrons at N atoms from Na_2EDTA, glutamic acid, and HNO_3 to reduce metals other than gold metal.

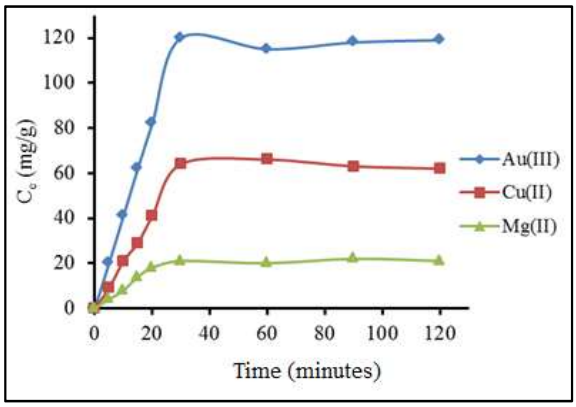

Figure 10. The desorption curve of the Au/Cu/Mg mixture by thiourea with variations in contact time

When compared, the metal ions Au(III), Cu(II), and Mg(II) are still more absorbed by Na_2EDTA and

glutamic acid because of the ability of the two absorbing agents to form a chelate with metal ions. Because the amount of gold adsorbed by $SH/Fe_3O_4@SiO_2$ is low, the gold that is desorbed from $SH/Fe_3O_4@SiO_2$ using nitric acid is also low.

Figure 10 shows that the longer the time for desorption, the more the percentage of Au(III), Cu(II), and Mg(II) is desorbed by thiourea. At the same time, it is seen that in the mixed Au/Cu/Mg system, the percentage of Au(III) desorbed is higher than that of Cu(II) and Mg(II). The average percentage of desorbed Au(III) was 60%, while the average Cu(II) that was desorbed was 20%. The maximum desorption of Au(III) started at 30 minutes, while Cu(II) and Mg(II) metals were maximally desorbed after 60 minutes. This result shows that thiourea can absorb Au(III) faster than Cu(II) and Mg(II) metals.

Table 3. Langmuir kinetics model on the desorption of Au(III),Cu(II), and Mg(II) metals in a multi-metal Au/Cu/Mg system

Metal	Rate constant (k)	Order
Au(III)	8.82 x 10^{-3} g mg^{-1} min^{-1}	Pseudo 2nd-order
Cu(II)	98.42 x 10^{-3} g mg^{-1} min^{-1}	Pseudo 2nd-order
Mg(II)	125.45 x 10^{-3} g mg^{-1} min^{-1}	Pseudo 2nd-order

Following the concept of HSAB (Hard and Soft Acids and Bases), Au(III) is a soft acid while Cu(II) and Mg(II) are hard acids, so the metal Au(III), which is a soft acid, can bind more strongly by the S group of thiourea which is a soft base. Therefore, the gold metal attached to the adsorbent can be recovered (desorbed) by the thiourea solution more than the copper or magnesium.

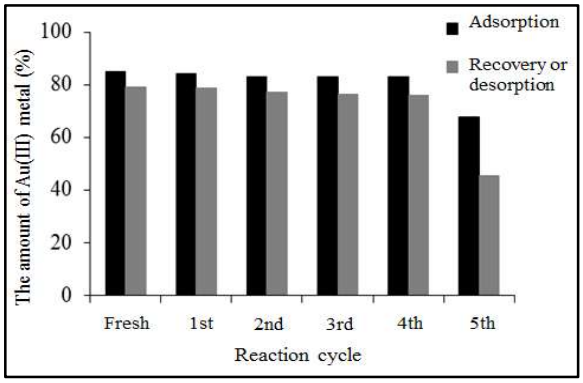

Figure 11. Adsorbent reuse $SH/Fe_3O_4@SiO_2$ for adsorption-desorption Au(III) in Au/Cu/Mg system

From Table 3, it can be seen that all the desorption reactions of Au(III), Cu(II), and Mg(II) tend to follow the pseudo-second-order reaction mechanism. When compared, the rate constant (k) to the desorption of Au(III) ions is lower than the Cu(II) and Mg(II) ions. The low value of the reaction rate constant (k) indicates that over time, to desorb each mg of Au(III) metal, a smaller amount of thiourea is required when compared to the amount of thiourea needed to desorb Cu(II) and Mg(II) metals. This indicates that thiourea will more easily adsorb Au(III) than the other two metals.

The stability of $SH/Fe_3O_4@SiO_2$ adsorbent was tested by reuse several times. Based on the results in Figure 11, it can be seen that on the 5th repetition, the amount of Au (III) that was successfully adsorbed or recovered decreased sharply. Thus, the $SH/Fe_3O_4@SiO_2$ adsorbent can be reused in the adsorption-desorption process of Au (III) in the Au/Cu/Mg mixture four times.

CONCLUSION

The silica coating on magnetite has been successfully carried out, in which the crystalline nature of magnetite has not changed. Characterization with XPS showed that the entire magnetite surface was coated with silica. Morphological analysis using SEM showed that the thickness of the silica blanket-covered on magnetite was about 5 nm with a round shape and smooth surface.

The metal ion Au(III), Cu(II), and Mg(II) will be adsorbed stably at pH = 3. In the mixed system Au/Cu/Mg multi-metal, the Au(III) percentage is adsorbed more easily (about 85%) by the $SH/Fe_3O_4@SiO_2$ adsorbent. This condition is based on the HSAB concept that Au(III) ions are softer metals than Cu (II) and Mg(II) in the order Au (III)> Cu(II)> Mg(II). The desorption of the three mixtures of metal ions was carried out with various desorption solutions. The results showed that Au (III) was more easily desorbed using a 7% thiourea solution in a 0.1 M HCl solution with a 79% desorption percentage. The $SH/Fe_3O_4@SiO_2$ adsorbent can be reused in the Au (III) adsorption-desorption process in the Au/Cu/Mg mixture four times.

REFERENCES

Adha, S. D. (2015). Pengaruh Konsentrasi Larutan HNO_3 Dan Waktu Kontak Terhadap Desorpsi Kadmium(Ii) Yang Terikat Pada Biomassa Azolla microphylla-Sitrat. *Jurnal Ilmu Kimia Universitas Brawijaya*, *1*(1), 636–642.

Anovitz, L. M., & Cole, D. R. (2015). Characterization and Analysis of Porosity and Pore Structures. *Reviews in Mineralogy and Geochemistry*, *80*(1), 61–164. https://doi.org/10.2138/rmg.2015.80.04

Bijang, C. M., Latupeirissa, J., & Ratuhanrasa, M. (2018). Biosorpsi Ion Logam Tembaga (Cu^{2+}) Pada Biosorben Rumput Laut Coklat (Padina australis). *Indonesian Journal of Chemical Research*, *6*(1), 26–37. https://doi.org/10.30598//ijcr.2018.6-cat

Ekmekyapar, F., Aslan, A., Bayhan, Y. K., & Cakici, A. (2012). Biosorption of Pb(II) by Nonliving Lichen Biomass of Cladonia rangiformis Hoffm. *International Journal of Environmental Research*, *6*(2), 417–424. https://doi.org/10.22059/ijer.2012.509

Ertan, E., & Gülfen, M. (2009). Separation of Gold(III) Ions from Copper(II) and Zinc(II) Ions Using Thiourea–Formaldehyde or Urea–Formaldehyde Chelating Resins. *Journal of Applied Polymer Science*, *111*(6), 2798–2805. https://doi.org/10.1002/app.29330

Hidayati, E. N., Suyanta, S., & Santosa, S. J. (2018). Pembuatan Nanopartikel Emas Melalui Proses Desorpsi-Reduktif $[AuCl_4]^-$ Teradsorpsi Pada Magnetit Mg/Al-NO_3 Hidrotalsit dengan Asam Glutamat. *BIMIPA*, *25*(1), 32–41.

Kurnia, K., Kaseside, M., & Iwamony, S. (2021). Study Microstructure of Fe_3O_4 Modification Using PEG 4000 form Iron Sand at Wari Ino Beach As A Biosensor Application. *Indonesian Journal of Chemical Research*, *8*(3), 168–171. https://doi.org/10.30598//ijcr.2021.8-kur

Lacoste-Bouchet, P., Deschênes, G., & Ghali, E. (1998). Thiourea Leaching of A Copper-Gold Ore Using Statistical Design. *Hydrometallurgy*, *47*(2), 189–203. https://doi.org/10.1016/S0304-386X(97)00043-1

Manuhutu, J., Nuryono, N., & Santosa, S. J. (2018). Desorpsi Ion Emas(III) Dalam Sistem Multilogam Au/Ni/Ag Dengan Menggunakan Variasi Tiourea-HCl. *Molluca Journal of Chemistry Education (MJoCE)*, *8*(1), 56–63. https://doi.org/10.30598/MJoCEvol8iss1pp56-63

Mujiyanti, D. R., Nisa, H., Rosyidah, K., Ariyani, D., & Abdullah, A. (2020). The Effect of Reaction Time on Viscosity and Density of Tetraethyl Orthosilicate from Silica Rice Husk Ash. *Indonesian Journal of Chemical Research*, *8*(1), 72–78. https://doi.org/10.30598/10.30598//ijcr.2020.8-dwi

Mulyasuryani, A., Ismuyanto, B., & Purwonugroho, D. (2012). Pemurnian Emas dari Bijih Emas Berkadar Rendah Menggunakan Karbon Aktif dari Arang Tempurung Kelapa. *Jurnal Natur Indonesia*, *14*(1), 1–6. https://doi.org/10.31258/jnat.14.1.1-6

Ngatijo, N., Gusti, D. R., Fadhilah, A. H., & Khairunnisah, R. (2020). Adsorben Magnetit Terlapis Dimerkaptosilika untuk Adsorpsi Anion Logam $[AuCl_4]^-$ dan $[Cr_2O_7]^-$. *Jurnal Riset Kimia*, *11*(2), 113–120. https://doi.org/10.25077/jrk.v11i2.353

Nuryono, N., Qomariyah, A., Kim, W., Otomo, R., Rusdiarso, B., & Kamiya, Y. (2019). Octyl and Propylsulfonic Acid co-Fixed Fe_3O_4@SiO_2 as A Magnetically Separable, Highly Active and Reusable Solid Acid Catalyst In Water. *Molecular Catalysis*, *475*, 110248. https://doi.org/10.1016/j.mcat.2018.11.019

Powell, K. J., Brown, P. L., Byrne, R. H., Gajda, T., Hefter, G., Sjöberg, S., & Wanner, H. (2007). Chemical speciation of environmentally significant metals with inorganic ligands Part 2: The Cu^{2+}-OH-, Cl^-, CO_3^{2-}, SO_4^{2-}, and PO_4^{3-} systems (IUPAC Technical Report). *Pure and Applied Chemistry*, *79*(5), 895–950. https://doi.org/10.1351/pac200779050895

Rahmayanti, M., Santosa, S. J., Sutarno, S., & Paweni, A. (2021). The Effectiveness of Magnetite Modified Gallic Acid Synthesized by Sonochemical Method As $AuCl_4^-$ Adsorbent-Reductor. *Indonesian Journal of Chemical Research*, *8*(3), 194–201. https://doi.org/10.30598//ijcr.2021.8-may

Sa'adah, S., Zaharah, T. A., & Shofiyani, A. (2018). Pengaruh Konsentrasi Na_2EDTA Terhadap Desorpsi Ce(IV) Pada Adsorben Kitosan-Karbon. *Jurnal Kimia Khatulistiwa*, *7*(4), 37–43.

Umaningrum, D., Mulyasuryani, A., & Sulistyarti, H. (2016). Pengaruh Konsentrasi Amonia Dalam Proses Pembentukan Kompleks $Au(NH_3)^{2+}$. *Jurnal Sains dan Terapan Kimia*, *6*(2), 112–117. https://doi.org/10.20527/jstk.v6i2.2111